Dalton Transactions

PAPER

View Article Online
View Journal | View Issue

Check for updates

Cite this: *Dalton Trans.*, 2019, **48**, 664

Expanding the limits of catalysts with low-valent main-group elements for the hydroboration of aldehydes and ketones using [L†Sn(II)][OTf] (L† = aminotroponate; OTf = triflate)†

Mahendra Kumar Sharma, [a] Mursaleem Ansari,[b] Pritam Mahawar,[a] Gopalan Rajaraman [b] and Selvarajan Nagendran *[a]

Received 12th July 2018,
Accepted 12th November 2018

DOI: 10.1039/c8dt02857e

rsc.li/dalton

A triflatostannylene [L†Sn(II)][OTf] (**2**) is reported here as an efficient catalyst with low-valent main-group element for the hydroboration of aldehydes and ketones (L† = aminotroponate). Using 0.025–0.25 mol% of compound **2**, hydroboration of various aldehydes and ketones is accomplished in 0.13–1.25 h at room temperature; the aliphatic aldehydes show an impressive TOF of around 30 000 h^{-1}. DFT calculations are performed to explore the mechanistic aspects of this reaction suggesting that the reaction proceeds *via* a stepwise pathway with hydridostannylene [L†Sn(II)H] (**2a**) as the active catalyst and the H atom transfer from the Sn–H bond to the carbonyl carbon being the rate determining step.

Introduction

In organic chemistry, the reduction of aldehydes and ketones is one of the most important transformations due to the requirement of the resultant alcohols for fine chemical production and natural product synthesis.[1] In this respect, the catalytic hydroboration of aldehydes and ketones using HBpin is a very significant reaction. This reaction in recent years has witnessed a surge in the use of main-group element compounds as catalysts.[2–25] Alkali metal hydridotriphenylborates [(L)M][$HBPh_3$] (M = Li (**A**), Na (**B**), K (**C**); L = tris{2-(dimethylamino)ethyl}amine) and magnesium hydridotriphenylborates [$Mg(thf)_6$][$HBPh_3$]$_2$ (**D**) were used as catalysts by the group of Okuda.[14,15] A benzamidinatocalcium iodide, [PhC(N^iPr)$_2$CaI] (**E**), isolated by Sen and co-workers was demonstrated as a useful catalyst.[16] Mulvey and co-workers employed lithium diamidodihydridoaluminate $(HMDS)_2AlH(\mu\text{-}H)Li(THF)_3$ (**F**) as a catalyst.[17] The groups of Hill and Stasch utilized magnesium based catalysts [L′Mg^{n}Bu] (**G**) and [(L″MgH)$_4$] (**H**) (L′ = HC(CMeNAr)$_2$, L″ = ArNHPPh$_2$; Ar = 2,6-^{i}Pr$_2$C$_6$H$_3$), respectively.[18,19] Group 13 element compounds that contain aluminium atoms, such as [L′AlH$_2$] (**I**) and [{(2,4,6-Me$_3$-C$_6$H$_2$)NC(Me)}$_2$(Me)(H)]AlH·(NMe$_2$Et) (**J**), were exploited by Roesky and Nembenna, respectively.[20,21] Jones and co-workers used group 14 element compounds, namely germylene L$^{\#}$GeH (**K**) and stannylene L$^{\#}$SnH (**L**) hydrides, as potential catalysts [(L$^{\#}$ = –N(Ar′)(SiPr$^i_3$), Ar′ = C$_6$H$_2${C(H)Ph$_2$}$_2$Pr^i-2,6,4)],[22] and germylene L*Ge: (**M**) was introduced by Zhao and co-workers {L* = CH[(C=CH$_2$)CMe][N(Ar)]$_2$} (Chart 1).[23] Wesemann *et al.* reported that intramolecularly stabilized germylene and stannylene PhCH(PPh$_2$)M(Ar*) [M = Ge (**N**), Sn (**O**)] can also be used as catalysts [Ar* = 2,6-(2,4,6-^{i}Pr$_3$C$_6$H$_2$)$_2$C$_6$H$_3$] (Chart 1).[24] An amidinate ligand stabilized dichlorosilane PhC(N^{t}Bu)$_2$SiHCl$_2$ (**P**) was found to be catalyst by the group of Sen.[25] 1,3,2-Diazaphospholene (HCN^{t}Bu)$_2$PH (**Q**), a group 15 element compound, was shown to be useful by Kinjo and co-workers.[26] As we have a long-standing interest in developing the applications of compounds with low-valent main-group elements, we researched on the use of base-stabilized stanny-

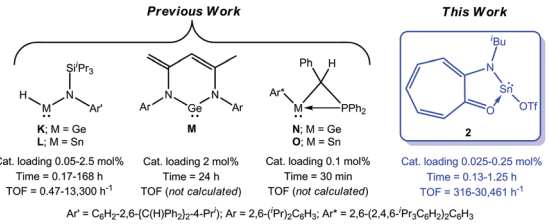

Chart 1 Catalytic hydroboration of aldehydes and ketones using compounds with low-valent main-group elements.

[a]*Department of Chemistry, Indian Institute of Technology Delhi, Hauz Khas, New Delhi 110 016, India. E-mail: sisn@chemistry.iitd.ac.in*
[b]*Department of Chemistry, Indian Institute of Technology Bombay, Powai, Mumbai 400 076, India*

†Electronic supplementary information (ESI) available: Characterization data of hydroboration products, copies of NMR spectra, and computational details. CCDC 1848467 and 1848468. For ESI and crystallographic data in CIF or other electronic format see DOI: 10.1039/c8dt02857e

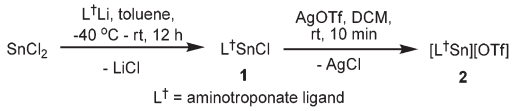

Scheme 1 Synthesis of triflatostannylene [L†Sn(II)][OTf] (**2**).

lenes as catalysts for the transformation under discussion. This exercise has resulted in identifying [L†Sn(II)][OTf] (**2**) as an efficient low-valent main-group catalyst for the hydroboration of aldehydes and ketones (L† = aminotroponate) (Chart 1).

Results and discussion

The reaction of $SnCl_2$ with a stoichiometric amount of L†Li gave yellow colored monochlorostannylene **1** in 85% yield (L† = aminotroponate) (Scheme 1).[27] The treatment of **1** with silver triflate in dichloromethane yielded triflatostannylene **2** quantitatively as an off-white solid (Scheme 1). Stannylenes **1** and **2** are soluble in benzene, toluene, diethyl ether, tetrahydrofuran, dichloromethane, and chloroform. They are stable at room temperature under an inert atmosphere and are characterized by NMR spectroscopic studies. In the ^{19}F NMR spectrum of compound **2**, a signal at −78 ppm due to the triflate moiety was seen. In the ^{119}Sn NMR spectra of compounds **1** and **2**, singlet resonances at −158 and −379 ppm were observed, respectively.

Single crystal X-ray diffraction studies confirm the molecular structures of stannylenes **1** and **2** (see the ESI† for details); they crystallized in the monoclinic and triclinic space groups $P2_1/c$ and $P\bar{1}$.[28] Both are dimeric due to intermolecular Sn···X interactions (X = Cl **1**, O **2**) (Fig. 1 and 2). The Sn···Cl (3.415 Å) and Sn···O (2.754 Å) bond lengths are longer than the Sn–Cl (2.531(2) Å) and Sn–$O(2)_{OTf}$ (2.305(2) Å) bonds in them, respectively. The latter bond in **2** is longer than the $Sn(1)–O(1)_{L^\dagger}$

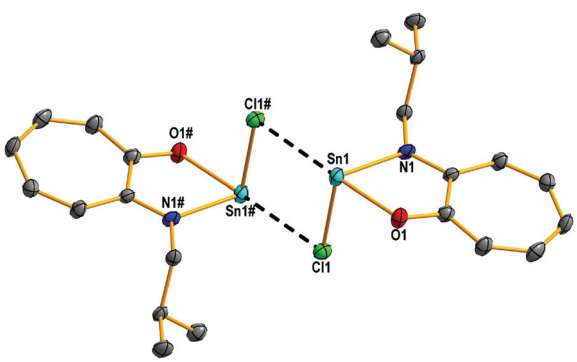

Fig. 1 Molecular structure of compound **1**. Thermal ellipsoids are drawn at the 40% probability level. All hydrogen atoms are deleted for clarity. Selected bond lengths (Å) and angles (°): Sn1–Cl1 2.531(2), Sn1–O1 2.127(4), Sn1–N1 2.183(5), Sn1–Cl1# 3.415(2); O1–Sn1–N1 74.12(2), O1–Sn1–Cl1 90.19(1), N1–Sn1–Cl1 91.86(14). Data collection temperature: 150 K.

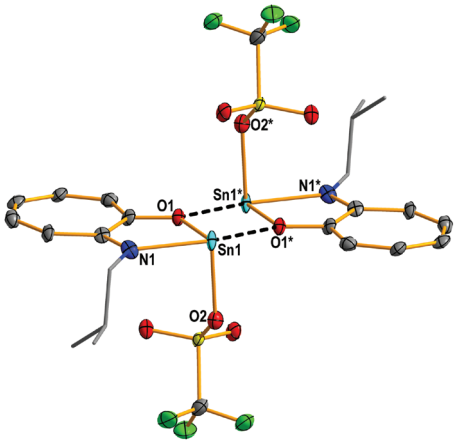

Fig. 2 Molecular structure of triflatostannylene **2**. Thermal ellipsoids are drawn at the 40% probability level. All hydrogen atoms are omitted for clarity. Selected bond lengths (Å) and angles (°): Sn1–O2 2.305(2), Sn1–O1 2.096(4), Sn1–N1 2.216(1), Sn1–O1* 2.754(2); O1–Sn1–N1 73.2(4), O1–Sn1–O2 88.6(3), N1–Sn1–O2 89.3(4). Data collection temperature: 100 K.

(2.096(4) Å) bond in it, and reveals the weakly coordinating nature of OTf with the tin atom.

To study the efficiency of the well-defined stannylenes **1** and **2** in the hydroboration of aldehydes and ketones using pinacolborane (HBpin), optimization experiments were carried out by using benzaldehyde as the substrate. When benzaldehyde reacted with 1.2 equiv. of HBpin in the absence of a catalyst at room temperature, no conversion was witnessed (entry 1, Table 1). The reactions between benzaldehyde and 1.2 equiv. of HBpin using 0.1 mol% of **1** and **2** in toluene took 40 and <5 min at room temperature to afford 97 and >99% con-

Table 1 Optimization of the reaction conditions for the hydroboration of benzaldehyde using HBpin in the presence of stannylene **1**/**2** as a catalyst

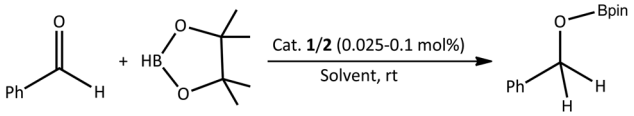

Entry	Cat. (mol%)	Solvent	Time (h)	% conversion
1	—	Toluene	12	Trace
2	**1** (0.1)	Toluene	0.66	97
3	**2** (0.1)	Toluene	<0.09	>99
4	**2** (0.025)	Toluene	0.33	>99
5	**2** (0.025)	Benzene	0.33	92
6	**2** (0.025)	THF	0.33	84
7	**2** (0.025)	CH_2Cl_2	0.33	70

Conditions: Benzaldehyde (1 mmol), HBpin (1.2 mmol), room temperature. % conversions were obtained by ^1H NMR spectroscopy; (a) for aldehydes, the integration of RC*H*O was compared with that of RCH_2(OBpin), (b) for methyl ketones, the integration of RC(O)CH_3 was compared with that of RC*H*(OBpin)(CH_3) or RCH(OBpin)(CH_3), and (c) for benzophenone, the integration of $(C_6H_5)_2CO$ (only the *ortho* protons of phenyl rings) was compared with that of $(C_6H_5)_2CH$(OBpin) or $(C_6H_5)_2$CH(OBpin) (only the *ortho* protons of phenyl rings).

version (entries 2 and 3, Table 1). This shows that stannylene **2** is far better than its chloro analogue **1**; for this reason only **2** was studied further. As the rate of hydroboration with 0.1 mol% of **2** was very high, to accurately monitor the reaction completion, the catalytic loading was reduced to 0.025 mol% in all the further studies with aldehydes. Under this catalytic loading, benzaldehyde took 0.33 h for >99% conversion (entry 4, Table 1). To choose the right solvent, 1.2 equiv. of HBpin was reacted with 1 equiv. of benzaldehyde for 0.33 h using 0.025 mol% of **2** in various common solvents other than toluene. The data obtained [benzene, 92% conversion (entry 5, Table 1); tetrahydrofuran, 84% conversion (entry 6, Table 1); and dichloromethane 70% conversion (entry 7, Table 1)] showed that toluene is the best solvent for this reaction. The TOF calculated for benzaldehyde under the optimized reaction conditions is 12 000 h^{-1} (entry 4, Table 1).

The substrate scope for catalyst **2** is discussed in Table 2. Aliphatic aldehydes, such as propionaldehyde and *n*-butyraldehyde, took only 0.13 h to yield the corresponding boronate esters providing a TOF of 30 461 h^{-1} (entries 1 and 2, Table 2). The hydroboration of *trans*-cinnamaldehyde afforded the hydroborylated product after 0.25 h with 99% conversion and showed a TOF of 15 840 h^{-1}. Furthermore, this occurred without affecting the C=C double bond and stands for the functional group tolerability of catalyst **2** (entry 3, Table 2). Aromatic aldehydes with one or more electron donating groups (OMe, Me) on the aryl ring were converted (% conversion above 98) into the corresponding boronate esters within 0.5 h with a TOF of around 7800 h^{-1} (entries 4–7, Table 2). The substrates with electron withdrawing groups (Cl, Br, NO_2) underwent smooth hydroboration reactions to afford the corresponding boronate esters faster (0.3–0.41 h) than the substrates with electron donating groups on the aryl ring (entries 8–10, Table 2). This can be realized from the TOF values also (9600–13 200 h^{-1}). Heterocyclic aldehydes, such as 2-thiophenecarboxaldehyde and 2-furaldehyde, were rapidly hydroborylated with a % conversion of 99 in 0.25 h with a TOF of 15 840 h^{-1} without the de-aromatization of the heterocyclic rings (entries 11 and 12, Table 2).

After aldehydes, the catalytic hydroboration of ketones was examined. Under 0.025 mol% loading of **2**, acetone took 1.6 h for 99% conversion indicating that the hydroboration of aliphatic ketones is relatively slower than that of aliphatic aldehydes. Therefore, for short reaction times, hydroboration of ketones was studied with 0.25 mol% of **2**. With this catalytic loading of **2**, near-quantitative conversion of acetone into the corresponding boronate ester was achieved in 0.16 h with a TOF of 2475 h^{-1} (entry 13, Table 2). Other aliphatic ketones,

Table 2 Hydroboration of aldehydes and ketones catalyzed by compound **2**[a]

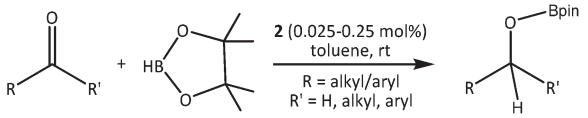

Entry	Substrate	Catalyst (mol%)	Time (h)	% conversion	TOF (h^{-1})
1	Propionaldehyde	0.025	0.13	>99	30 461
2	*n*-Butyraldehyde	0.025	0.13	>99	30 461
3	*trans*-Cinnamaldehyde	0.025	0.25	99	15 840
4	4-Methoxylbenzaldehyde	0.025	0.50	99	7920
5	2-Methylbenzaldehyde	0.025	0.50	98	7840
6	4-Methylbenzaldehyde	0.025	0.50	99	7920
7	2,4,6-Trimethylbenzaldehyde	0.025	0.50	98	7840
8	4-Chlorobenzaldehyde	0.025	0.30	99	13 200
9	4-Bromobenzaldehyde	0.025	0.30	99	13 200
10	3-Nitrobenzaldehyde	0.025	0.41	99	9658
11	2-Thiophenecarboxaldehyde	0.025	0.25	99	15 840
12	2-Furaldehyde	0.025	0.25	99	15 840
13	Acetone	0.25	0.16	99	2475
14	4-Phenyl-2-butanone	0.25	0.16	99	2475
15	2-Pentanone	0.25	0.16	99	2475
16	Methylisopropylketone	0.25	0.16	99	2475
17	Acetophenone	0.25	0.41	99	965
18	4-Methylacetophenone	0.25	0.41	99	965
19	4-Methoxyacetophenone	0.25	0.41	98	956
20	4-Fluroacetophenone	0.25	0.33	99	1200
21	4-Chloroacetophenone	0.25	0.33	99	1200
22	4-Bromoacetophenone	0.25	0.33	99	1200
23	4-Nitroacetophenone	0.25	0.33	99	1200
24	2-Chloroacetophenone	0.25	0.33	98	1187
25	3-Bromoacetophenone	0.25	0.50	98	784
26	Benzophenone	0.25	1.25	99	316

[a] Conditions: Aldehyde/ketone (1 mmol), HBpin (1.2 mmol). % conversions were obtained according to the procedure mentioned in the footnote of Table 1.

such as 4-phenyl-2-butanone, 2-pentanone, and methylisopropylketone, could also be converted into the corresponding hydroborylated products within 0.16 h to afford a % conversion of 99 with a TOF of 2475 h^{-1} (entries 14–16, Table 2). Then, ketones with one aromatic group on the carbonyl carbon were studied. It was found that they require longer reaction times than the aforementioned aliphatic ketones. Thus, a reaction of acetophenone with HBpin took 0.41 h for almost quantitative conversion with a TOF of 965 h^{-1} (entry 17, Table 2). Aromatic ketones with electron donating substituents on the phenyl ring, such as 4-methylacetophenone and 4-methoxyacetophenone, underwent hydroborylation similar to acetophenone and produced the corresponding hydroborylated products in 0.41 h with a % conversion of 98 (entries 18 and 19, Table 2). Aromatic ketones with electron withdrawing substituents (such as 4-fluroacetophenone, 4-chloroacetophenone, 4-bromoacetophenone, 4-nitroacetophenone, and 2-chloroacetophenone) on the aryl ring gave a % conversion around 98 after 0.33 h with a TOF of 1200 h^{-1} (entries 20–24, Table 2). In contrast, 3-bromoacetophenone required 0.50 h to produce 98% conversion into the desired boronate ester with a TOF of 784 h^{-1} (entry 25, Table 2). Ketones with two aromatic groups on the carbonyl carbon, namely, benzophenone, took 1.25 h for 99% conversion (entry 26, Table 2) with a TOF of 316 h^{-1}. The TOF for this substrate is lower than those of the ketones with one aromatic group on the carbonyl carbon.

The efficiency of catalyst **2** is compared with other main group catalysts **A**, **E**, **K**, **L**, and **Q** for which the TOF values are reported. For this purpose, the TOF values obtained for a few of the standard substrates, such as propionaldehyde, *n*-butyraldehyde, benzaldehyde, acetophenone, benzophenone, and cinnamaldehyde, are considered (Table 3). To the best of our knowledge, the current leading main group catalytic system for the hydroboration of aldehydes/ketones is **A**.[14] As shown in Table 3, with the exception of cinnamaldehyde, the efficiency of **A** with respect to all the other substrates is better than that of **2**.

Chemoselective hydroboration using compound **2** was also screened (Scheme 2). The reaction of equimolar amounts of benzaldehyde, acetophenone, and HBpin with 0.025 mol% of **2** (eqn (1), Scheme 2) resulted in the exclusive hydroboration of benzaldehyde only with 99% conversion after 0.33 h. Repetition of this reaction with activated ketones, such as 4-bromoacetophenone instead of acetophenone (eqn (1), Scheme 2), also afforded the same result. These reactions offer support to the intermolecular chemoselectivity achievable using catalyst **2**. The intramolecular chemoselective hydroboration of aldehydes in the presence of other functional groups, namely ketone, ester, and amide, was also investigated (eqn (2)–(4), Scheme 2). In all these reactions, only the aldehydic groups of 4-acetylbenzaldehyde, methyl 4-formylbenzoate, and 4-acetamidobenzaldehyde were hydroborylated within 0.33 h without affecting the keto, ester, and amide functional groups in them, respectively.

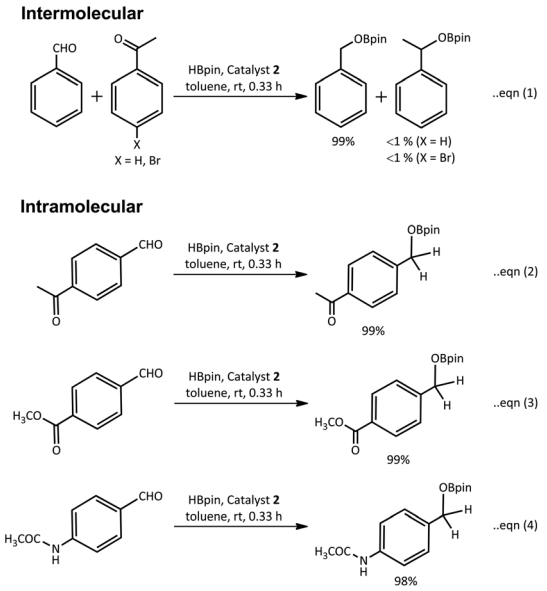

Scheme 2 Inter- and intramolecular chemoselective hydroboration of aldehydes in the presence of other functional groups using **2** (0.025 mol%). % conversions given below the structures of the hydroborylated products were obtained according to the procedure mentioned in the footnote of Table 1.

To understand the mechanism of hydroboration of aldehydes and ketones using **2**, DFT calculations were carried out using benzaldehyde as the substrate. Two mechanistic pathways were studied: (a) concerted (see Scheme S1 in the ESI;† Fig. 3) and (b) stepwise (see Scheme S2 in the ESI;† Fig. 4). In the concerted pathway, catalyst **2** initially interacts with benzaldehyde to give **2a′** ($Sn–O_C$ = 2.980 Å) and its formation is computed to be endothermic by 16.6 kcal mol^{-1} (weak

Table 3 Comparison of the TOF values obtained (for a few of the standard substrates) using **2** with other main group catalysts **A**, **E**, **K**, **L**, and **Q**

	Catalyst[a]					
Substrate	**2**	**A**	**E**	**K**	**L**	**Q**
Propionaldehyde	30 461 (>99)	—	—	2000 (>99)	≥13 300 (>99)	—
n-Butyraldehyde	30 461 (>99)	≥60 000 (≥99)	—	—	—	—
Benzaldehyde	12 000 (99)	≥60 000 (≥99)	249 (83)	67 (>99)	800 (>99)	404 (>99)
Acetophenone	965 (99)	≥60 000 (≥99)	9.5 (95)	—	—	—
Benzophenone	316 (99)	66 600 (≥99)	8.6 (86)	1.7 (>99)	80 (>95)	1.8 (>99)
Cinnamaldehyde	15 840 (99)	210 (≥99)	69 (91)	—	—	—

[a] % conversions/yields are given in brackets.

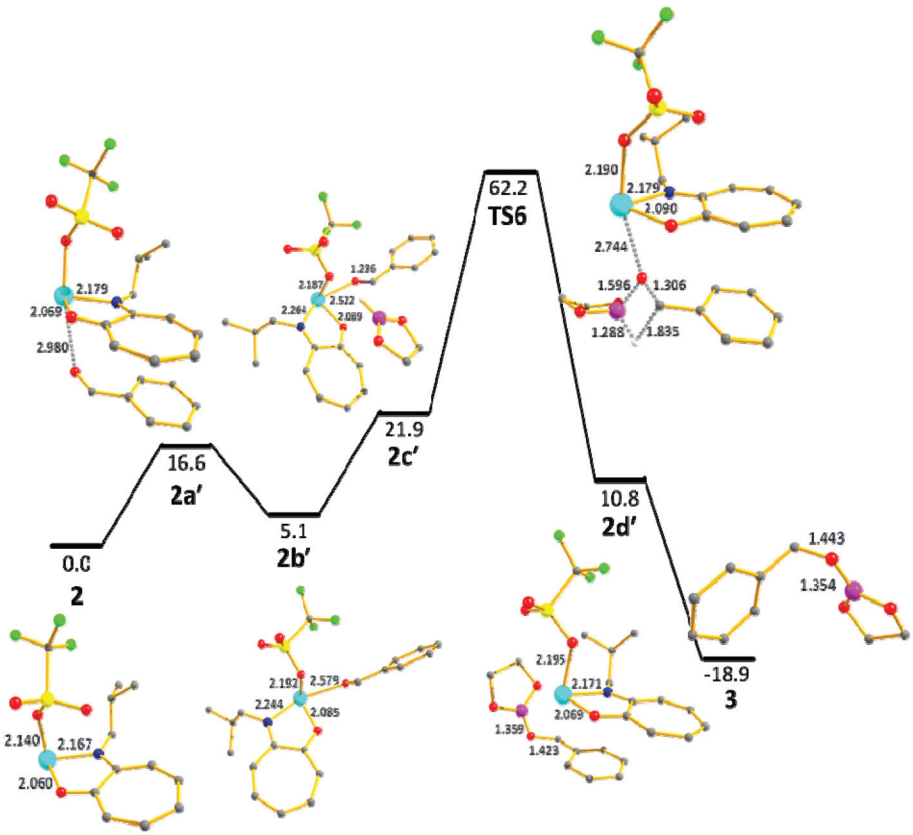

Fig. 3 Computed (B3LYP-D2/def2-TZVP) free energy profile for the concerted mechanism proposed for the catalytic hydroboration of benzaldehyde using HBpin′ in the presence of catalyst **2** (HBpin′ = a model compound with all the methyl groups of HBpin replaced by hydrogen atoms). Free energy (kcal mol^{-1}) and selected bond lengths (Å) are also shown. All hydrogen atoms (except B–H) are omitted for clarity.

complex formation) (O_C represents the oxygen of the aldehyde). Then, the nucleophilic carbonyl oxygen of benzaldehyde coordinates with the electrophilic tin(II) atom to form **2b′** (Sn–O_C = 2.579 Å); this leads to stabilization in comparison with **2a′**. In the next step, **2b′** reacts with HBpin′ to generate **2c′**; the formation of this species is endothermic. **2c′** then gets transformed to **2d′** (which is an adduct between catalyst **2** and the hydroborylated product **3**) through a transition state **TS6** where σ-bond metathesis occurs. The activation energy of the **TS6** is 62.2 kcal mol^{-1} and it is characterized by a single imaginary frequency of −528 cm^{-1}. **TS6** involves a four-membered boracycle weakly attached to the tin atom through the carbonyl oxygen atom. The Sn–O, C–O, and B–H bonds in **TS6** are elongated to 2.744, 1.306, and 1.288 Å from the corresponding values of 2.522, 1.236, and 1.186 Å seen in **2c′**, respectively. But the O–B and C–H bonds in **2c′** (4.725 Å and 3.406 Å) are shortened to 1.596 and 1.835 Å in **TS6**, as anticipated, respectively. These changes in the bond lengths indicate that the breaking of the π-bond of the C=O group and the formation of the O–B bond take place simultaneously. Furthermore, as one would expect for the bond formation between the B and O atoms, the Mulliken charges on these atoms are found to be 0.85 and −0.33 (in the **TS6**), respectively. In the next step, **2d′** affords the hydroborylated product **3** and catalyst **2**. The formation of **3** is computed to be exothermic by −18.9 kcal mol^{-1}. Due to the prohibitively high barrier height for the formation of **TS6** from **2**, the concerted pathway can be ruled out.

In the stepwise pathway, the formation of a hydridostannylene **2a** as an active catalyst from the reaction of precatalyst **2** with HBpin′ was considered (Scheme S2 in the ESI;† Fig. 4) and the formation of **2a** is endothermic by 13.7 kcal mol^{-1} from compound **2**. Interaction between the nucleophilic carbonyl oxygen of benzaldehyde and the electrophilic tin(II) atom of **2a** leads to a weak complex **2b** followed by the coordination of the oxygen atom of benzaldehyde to the tin atom of **2b** to result in **2c**. This is indicated by the reduction in the Sn···O_C bond length from 2.953 Å (in **2b**) to 2.691 Å (in **2c**). The formations of **2b** and **2c** are endothermic by 11.2 and 9.3 kcal mol^{-1} from catalyst **2a**, respectively; this endothermicity is correlated with the energy required to form the Sn···O_C bond. Then, the hydrogen atom transfer from **2c** to benzaldehyde leads to an alkoxystannylene intermediate **2d** through a transition state **TS1**. The formation of **TS1** is the rate limiting step with a small energy barrier of 26.9 kcal mol^{-1} from **2a** and it is characterized by an imaginary frequency of −499 cm^{-1}. The **TS1** involves a four-membered stannacycle, where the hydrogen atom interacts with the electrophilic carbonyl carbon atom and the nucleophilic carbonyl oxygen atom makes bonding interaction with

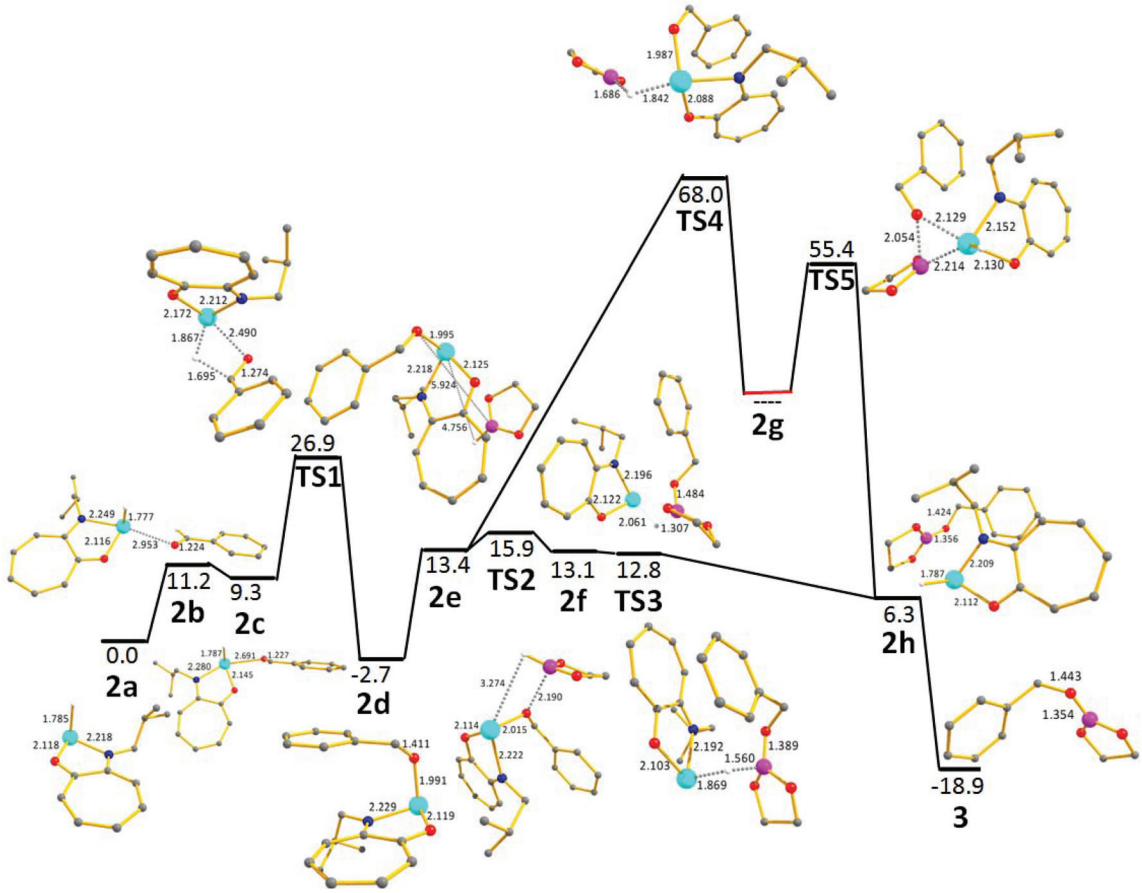

Fig. 4 Computed (B3LYP-D2/def2-TZVP) free energy profile for the plausible stepwise mechanism proposed for the catalytic hydroboration of benzaldehyde using HBpin′ in the presence of active catalyst **2a**. The formation of compound **2a** is visualized through the reaction of precatalyst **2** with HBpin′. Free energy (kcal mol^{-1}) and selected bond lengths (Å) are also shown. All hydrogen atoms (except Sn–H and B–H) are omitted for clarity.

the electrophilic tin atom of **2c**. Accordingly in **TS1**, the Sn–H (1.867 Å) and C–O (1.274 Å) bonds are elongated in comparison with the former (1.787 Å) and latter (1.227 Å) bonds in **2c**. At the same time, the Sn···O$_C$ bond is shortened to 2.490 Å from the corresponding value of 2.691 Å in **2c**. These indicate the weak interaction of the nucleophilic hydrogen atom (computed Mullikan charge Q_H = −0.24 e) with the carbonyl carbon atom (Q_C = 0.11 e). The formation of alkoxystannylene **2d** is slightly exothermic with respect to **2a**. The interaction of **2d** with HBpin′ then leads to a weak complex **2e**, and the formation of **2h** (an adduct between active catalyst **2a** and the hydroborylated product **3**) from **2e** was visualized through two different possibilities. The first possibility is through **TS2**, where the B atom of HBpin′ interacts with the alkoxide oxygen atom of **2e**. The calculated barrier height for the formation of **TS2** is 2.5 kcal mol^{-1} from **2e**. **TS2** is a four membered stannacycle and its structure clearly indicates the partial formation of the O···B bond (2.190 Å against 5.924 Å in **2e**). For the formation of the bond between B and O atoms, the charges on them are also conductive (0.80 and −0.61 respectively). Strengthening of this interaction results in intermediate **2f**, where the B–O bond is almost fully formed. From **2f**, hydrogen atom transfer takes place through **TS3** and results in **2h**. The energy of **TS3** is nearly the same as that of **2f** suggesting a barrierless process. In the second possibility, hydride transfer from the B–H bond of HBpin′ to the tin atom of **2e** proceeds through **TS4** to afford an intermediate **2g**. **TS4** has a prohibitively high energy barrier of 68.0 kcal mol^{-1}; and it clearly indicates partial B–H bond breakage and Sn···H bond formation. Thus, the B–H bond in **TS4** is elongated (1.686 Å) in comparison with that in **2e** (1.186 Å), and the Sn···H bond is strengthened (1.842 Å) relative to that in **2e** (4.756 Å). But our attempts to obtain intermediate **2g** were unsuccessful, and the exact barrier height for this process could not be estimated. In the next step, **2g** should lead to **2h** through the transition state **TS5**. In **TS5**, interaction between the boron atom of HBpin′ and the alkoxide oxygen atom occurs and this step also has a prohibitive kinetic barrier of 55.4 kcal mol^{-1}. Thus, our calculations clearly indicate that (from **2e**) the initial hydrogen atom transfer to the tin(II) centre followed by the O–B bond formation as seen in the second possibility is highly unfavourable. Instead, the calculations clearly reveal that (from **2e**) the initial O–B bond formation followed by the hydrogen atom transfer to the tin(II) atom as in the case of the first possibility is highly feasible.

Therefore, the formation of **2h** from **2e** should take the path as described in the first possibility. Finally, **2h** affords the free catalyst **2a** and the hydroborylated product **3**. The formation of the hydroborylated product **3** from **2h** is exothermic by −18.9 kcal mol^{-1}, and therefore its formation serves as a thermodynamic sink for the overall reaction to take place. The presence of a hydride on the tin(II) atom in **2a** eases out the energetics of the process and makes the stepwise pathway a probable one. Jones and co-workers proposed a similar stepwise pathway for the catalytic hydroboration of aldehydes and ketones using a two-coordinate stannylene $L^{\#}SnH$ (**L**).[22]

Conclusions

To conclude, a base stabilized triflatostannylene **2** is demonstrated as an efficient catalyst for the hydroboration of various aldehydes and ketones with a very good functional group tolerance. Catalyst **2** is also promising for the chemoselective hydroboration of aldehydes in the presence of keto, ester, and amide groups. DFT calculations suggest that a stepwise pathway that involves hydridostannylene **2a** as an active catalyst is more preferred over a concerted pathway that uses compound **2** as the catalyst.

Encouraged by the efficiency of compound **2** for the hydroboration of aldehydes and ketones, we are currently checking its potential to cyanosilylate aldehydes and ketones using trimethylsilyl cyanide (TMSCN). This should be interesting, as to the best of our knowledge there is no example of a tin compound that can catalyze the cyanosilylation of aldehydes and ketones. The initial results obtained are highly encouraging; further details will be published elsewhere soon.

Experimental section

General information

All the experiments were performed under an atmosphere of dry N_2 using glove box [GP(Concept)-T2, Jacomex work station] techniques. The temperature inside the glove box (room temperature) was around 43 °C. Hexane, THF, benzene, and toluene were dried using conventional procedures. The lithium salt of aminotroponate ($L^{\dagger}Li$; $L^{\dagger}$ = aminotroponate) was synthesized according to the literature procedure.[27] $SnCl_2$ and AgOTf were purchased from Sigma Aldrich and used as received without any further purification. $CDCl_3$ for NMR spectroscopic analysis was obtained from Sigma Aldrich and dried over molecular sieves (4 Å). The melting points of compounds **1** and **2** were recorded using a Unitech Sales digital melting point apparatus by sealing the samples in glass capillaries and the reported values are uncorrected. Elemental analyses were carried out using a PerkinElmer CHN analyzer. ^1H, ^{13}C, and ^{119}Sn NMR spectra were recorded on a 300 MHz Bruker Topspin/400 MHz Bruker Topspin/400 MHz JEOL JNM-ECA NMR spectrometer. The chemical shifts δ are reported in ppm and are referenced internally to residual solvent (^1H NMR) and solvent (^{13}C NMR) resonances. For ^{119}Sn NMR spectroscopic studies, Me_4Sn was used as an external reference.

Synthesis of chlorostannylene 1

$L^{\dagger}Li$ (2.00 g, 10.91 mmol) and toluene (30 mL) were taken in a Schlenk flask. This flask was kept inside the refrigerator (at −40 °C) in the glove box for 1 h. Then, it was taken out and $SnCl_2$ (2.07 g, 10.91 mmol) was added to it and the mixture stirred for 12 h at room temperature. The reaction mixture was then filtered using a G4 frit containing Celite. Removal of the solvent from the filtrate under reduced pressure gave a yellow solid. It was washed with hexane (10 mL) and dried under vacuum to afford an analytically pure sample of compound **1**. Single crystals of compound **1** suitable for X-ray diffraction studies were obtained from its saturated toluene solution at −28 °C. Yield: 3.05 g, 85%. Mp: 121 °C (decom.). Anal. calcd for $C_{11}H_{14}ClNOSn$ (M = 330.40): C, 39.99; H, 4.27; N, 4.24. Found: C, 39.83; H, 4.09; N, 4.19. ^1H NMR (300 MHz, $CDCl_3$): δ 1.08 (d, $^3J_{HH}$ = 6 Hz, 6H, $CH(CH_3)_2$), 2.17–2.26 (m, 1H, $CH(CH_3)_2$), 3.45 (d, $^3J_{HH}$ = 6 Hz, 2H, CH_2), 6.90 (t, $^3J_{HH}$ = 9.9 Hz, 1H, C*H*), 7.02 (d, $^3J_{HH}$ = 12.0 Hz, 1H, C*H*), 7.28 (t, $^3J_{HH}$ = 10.2 Hz, 2H, C*H*), 7.34–7.45 (m, 1H, C*H*). $^{13}C\{^1H\}$ NMR (75 MHz, $CDCl_3$): δ 21.49 ($CH(CH_3)_2$), 29.19 ($CH(CH_3)_2$), 55.68 (CH_2), 120.61 (C_{Ar}), 123.99 (C_{Ar}), 126.41 (C_{Ar}), 137.38 (C_{Ar}), 137.83 (C_{Ar}), 164.31 (C_{Ar}), 176.13 (C_{Ar}). $^{119}Sn\{^1H\}$ NMR (111.88 MHz, $CDCl_3$): δ −158.42 ppm.

Synthesis of triflatostannylene 2

A solution of compound **1** (3.00 g, 9.07 mmol) in dichloromethane (30 mL) was prepared in a Schlenk flask using the dichloromethane taken out from the refrigerator of the glove box. AgOTf (2.33 g, 9.07 mmol) was added to it and the reaction mixture was stirred for 10 min at room temperature. The reaction mixture was then filtered using a G4 frit containing Celite. Removal of the solvent under reduced pressure from the filtrate gave an off-white solid. It was washed with hexane (15 mL) and dried under vacuum to give an analytically pure sample of compound **2**. Yield: 3.95 g, 98%. Mp: 117 °C (decom.). Anal. calcd for $C_{12}H_{14}F_3NO_4SSn$ (M = 444.01): C, 32.46; H, 3.18; N, 3.15. Found: C, 32.29; H, 3.27; N, 3.25. ^1H NMR (400 MHz, $CDCl_3$): δ 1.09 (d, $^3J_{HH}$ = 6.4 Hz, 6H, $CH(CH_3)_2$), 2.19–2.28 (m, 1H, $CH(CH_3)_2$), 3.60 (s, $^3J_{HH}$ = 7.2 Hz, 2H, CH_2), 7.34 (t, $^3J_{HH}$ = 9.2 Hz, 2H, C*H*), 7.62–7.67 (m, 2H, C*H*), 7.77 (t, $^3J_{HH}$ = 9.6 Hz, 1H, C*H*). $^{13}C\{^1H\}$ NMR (100 MHz, $CDCl_3$): δ 21.14 ($CH(CH_3)_2$), 28.40 ($CH(CH_3)_2$), 53.95 (CH_2), 121.27 (C_{Ar}), 124.81 (C_{Ar}), 130.76 (C_{Ar}), 139.06 (C_{Ar}), 140.32 (C_{Ar}), 162.31 (C_{Ar}), 173.98 (C_{Ar}). $^{19}F\{^1H\}$ NMR (376.46 MHz, $CDCl_3$): δ −78.04. $^{119}Sn\{^1H\}$ NMR (149 MHz, $CDCl_3$): δ −379.26 ppm.

General procedure for the hydroboration of aldehydes and ketones

To a solution of aldehyde/ketone (1 mmol) and HBpin (1.2 mmol) in toluene (1 mL), catalyst **2** (0.025–0.25 mol%) was added. The resulting solution was stirred for an appropriate time period at room temperature. The solvent was then

removed under reduced pressure, and the resultant product was characterized by ^{1}H and ^{13}C NMR spectroscopy. As mentioned in the footnote of Table 1, % conversions were obtained by ^{1}H NMR spectroscopy; (a) for aldehydes, the integration of RC*H*O was compared with that of RCH_2(OBpin), (b) for methyl ketones, the integration of RC(O)CH_3 was compared with that of RC*H*(OBpin)(CH$_3$) or RCH(OBpin)(CH_3), and (c) for benzophenone, the integration of (C$_6H_5$)$_2$CO (only the *ortho* protons of phenyl rings) was compared with that of (C$_6$H$_5$)$_2$C*H*(OBpin) or (C$_6H_5$)$_2$CH(OBpin) (only the *ortho* protons of phenyl rings). A sample calculation of % conversion is shown in Fig. S72.† The chemical shift (δ) values (in ppm) of RC*H*O, RC(O)CH_3, and (C$_6H_5$)$_2$CO (only the *ortho* protons of phenyl rings) in the substrates (used in the present study) are presented in Table S3.† *Note*: The substrates propionaldehyde, *n*-butyraldehyde, acetone, 2-pentanone, and methylisopropylketone have volatilities equivalent to or greater than that of toluene. To find out the % conversions in the reactions involving these substrates, the ^{1}H NMR spectra of the reaction mixtures were recorded without the removal of any volatiles; 0.1 mL of the reaction mixtures was taken in NMR tubes with 0.4 mL of CDCl$_3$ and the ^{1}H NMR spectra were recorded. The resultant NMR spectra (that contain toluene signals) are provided in the ESI (Fig. S11, S14, S40, S45, and S48†). Even for the substrates having volatilities lower than that of toluene, their loss (if any) during the removal of the volatiles under reduced pressure can make the reported % conversions erroneous. To show that this is not happening, five such substrates having high boiling points (162–210 °C) (such as benzaldehyde, 4-methylbenzaldehyde, 2-thiophenecarboxaldehyde, 2-furaldehyde, and 4-fluroacetophenone) (see Table S2† for the boiling point data of the substrates) were chosen and their catalytic hydroboration reactions were carried out. After the completion of the reactions, as done for the volatile substrates (*vide supra*), the ^{1}H NMR spectra of the reaction mixtures were recorded without the removal of any volatiles. The obtained spectra along with toluene signals (see Fig. S8, S23, S34, S37, and S57†) reveal the absence of substrate peaks. Furthermore, these spectra are comparable to the corresponding spectra recorded on the crude products obtained after the removal of all the volatiles. On the basis of these data, it can safely be concluded that there is no loss of substrates during evaporation. Although all the reported spectra are for the crude hydroborylated products, impurities (such as residual HBPin, catalyst, and starting material) are not seen in them due to the following reasons: (i) the evaporation process helped in removing the excess HBpin, (ii) the catalyst was used in very small quantities in comparison with the substrates, and (iii) the % conversions with respect to most of the substrates are high, respectively.

X-ray crystal structure determination of compounds 1 and 2

The data for compounds **1** and **2** were collected through a Bruker SMART APEX diffractometer equipped with a 3-axis goniometer (Table S1†).[29] The crystals were covered with a cryoprotectant (paratone–N) and mounted on a glass capillary. The data were collected under a steady flow of cold dinitrogen using Mo Kα radiation (λ = 0.71073 Å). The data were integrated using SAINT, and an empirical absorption correction was applied using SADABS.[30] The structures were solved by direct methods and refined by full matrix least-squares on F^2 using the SHELXTL software.[31,32] All non-hydrogen atoms were refined anisotropically. The positions of the hydrogen atoms were fixed according to a riding model and were refined isotropically.

Author contributions

All the experimental studies were performed by M. K. S., who also wrote the experimental part of the manuscript. M. A. carried out the theoretical studies, and drafted the theoretical portion of the manuscript. P. M. assisted M. K. S. to carry out some of the experiments. The experimental and theoretical write-ups of the manuscript were corrected by S. N. and G. R., respectively.

Conflicts of interest

There are no conflicts to declare.

Acknowledgements

M. K. S., P. M., and M. A. thank the Indian Institute of Technology Delhi (IITD), New Delhi, and Indian Institute of Technology Bombay (IITB), Mumbai, India, for research fellowships, respectively. S. N. thanks the SERB, Department of Science and Technology (DST), New Delhi, India, for funding (SB/S1/IC-46/2013) and the DST-FIST for establishing single crystal X-ray diffraction (SR/FST/CSII-027/2014) and HRMS (SR/FST/CS-1-195/2008) facilities in the Department of Chemistry, IIT Delhi. G. R. thanks the INSA (Indian National Science Academy) and the SERB (EMR/2014/000247) for funding. Dedicated to Prof. Mitsuo Kira on the occasion of his 75th birthday.

Notes and references

1 (*a*) A. Fürstner, *Angew. Chem., Int. Ed.*, 2014, **53**, 8587–8598; (*b*) R. A. Shenvi, D. P. O'Malley and P. S. Baran, *Acc. Chem. Res.*, 2009, **42**, 530–541.
2 T. J. Hadlington, M. Driess and C. Jones, *Chem. Soc. Rev.*, 2018, **47**, 4176–4197.
3 S. K. Mandal and H. W. Roesky, *Acc. Chem. Res.*, 2012, **45**, 298–307.
4 (*a*) A. Harinath, J. Bhattacharjee, H. P. Nayekb and T. K. Panda, *Dalton Trans.*, 2018, **47**, 12613–12622; (*b*) H. Stachowiak, J. Kaźmierczak, K. Kucińskia and G. Hreczycho, *Green Chem.*, 2018, **20**, 1738–1742; (*c*) R. E. Mulvey, J. Okuda, L. E. Lemmerz, R. McLellan, N. R. Judge, A. R. Kennedy, S. A. Orr, M. Uzelac, E. Hevia

and S. D. Robertson, *Chem. – Eur. J.*, 2018, **24**, 9940–9948; (*d*) V. A. Pollard, M. Ángeles Fuentes, A. R. Kennedy, R. McLellan and R. E. Mulvey, *Angew. Chem., Int. Ed.*, 2018, **57**, 10651–10655.
5 G. I. Nikonov, *ACS Catal.*, 2017, **7**, 7257–7266.
6 (*a*) C. C. Chong and R. Kinjo, *ACS Catal.*, 2015, **5**, 3238–3259; (*b*) K. Revunova and G. I. Nikonov, *Dalton Trans.*, 2015, **44**, 840–866.
7 J. R. Lawson, L. C. Wilkins and R. L. Melen, *Chem. – Eur. J.*, 2017, **23**, 10997–11000.
8 B. Prashanth, M. Bhandari, S. Ravi, K. R. Shamasundar and S. Singh, *Chem. – Eur. J.*, 2018, **24**, 4794–4799.
9 M. K. Bisai, T. Das, K. Vanka and S. S. Sen, *Chem. Commun.*, 2018, **54**, 6843–6846.
10 (*a*) H. Osseili, D. Mukherjee, T. P. Spaniol and J. Okuda, *Chem. – Eur. J.*, 2017, **23**, 14292–14298; (*b*) M. Ma, J. Li, X. Shen, Z. Yu, W. Yao and S. A. Pullarkat, *RSC Adv.*, 2017, **7**, 45401–45407; (*c*) D. Franz, L. Sirtl, A. Pöthig and S. Inoue, *Z. Anorg. Allg. Chem.*, 2016, **642**, 1245–1250.
11 I. P. Query, P. A. Squier, E. M. Larson, N. A. Isley and T. B. Clark, *J. Org. Chem.*, 2011, **76**, 6452–6456.
12 (*a*) S. Yadav, S. Pahar and S. S. Sen, *Chem. Commun.*, 2017, **53**, 4562–4564; (*b*) A. J. Blake, A. Cunningham, A. Ford, S. J. Teat and S. Woodward, *Chem. – Eur. J.*, 2000, **6**, 3586–3594; (*c*) A. Ford and S. Woodward, *Angew. Chem., Int. Ed.*, 1999, **38**, 335–336.
13 K. Manna, P. Ji, F. X. Greene and W. Lin, *J. Am. Chem. Soc.*, 2016, **138**, 7488–7491.
14 D. Mukherjee, H. Osseili, T. P. Spaniol and J. Okuda, *J. Am. Chem. Soc.*, 2016, **138**, 10790–10793.
15 D. Mukherjee, S. Shirase, T. P. Spaniol, K. Mashima and J. Okuda, *Chem. Commun.*, 2016, **52**, 13155–13158.
16 S. Yadav, S. Pahar and S. S. Sen, *Chem. Commun.*, 2017, **53**, 4562–4564.
17 V. A. Pollard, S. A. Orr, R. McLellan, A. R. Kennedy, E. Hevia and R. E. Mulvey, *Chem. Commun.*, 2018, **54**, 1233–1236.
18 M. Arrowsmith, T. J. Hadlington, M. S. Hill and G. Kociok-Köhn, *Chem. Commun.*, 2012, **48**, 4567–4569.
19 L. Fohlmeister and A. Stasch, *Chem. – Eur. J.*, 2016, **22**, 10235–10246.
20 Z. Yang, M. Zhong, X. Ma, S. De, C. Anusha, P. Parameswaran and H. W. Roesky, *Angew. Chem., Int. Ed.*, 2015, **54**, 10225–10229.
21 V. K. Jakhar, M. K. Barman and S. Nembenna, *Org. Lett.*, 2016, **18**, 4710–4713.
22 T. J. Hadlington, M. Hermann, G. Frenking and C. Jones, *J. Am. Chem. Soc.*, 2014, **136**, 3028–3031.
23 Y. Wu, C. Shan, Y. Sun, P. Chen, J. Ying, J. Zhu, L. Liu and Y. Zhao, *Chem. Commun.*, 2016, **52**, 13799–13802.
24 J. Schneider, C. P. Sindlinger, S. M. Freitag, H. Schubert and L. Wesemann, *Angew. Chem., Int. Ed.*, 2017, **56**, 333–337.
25 M. K. Bisai, S. Pahar, T. Das, K. Vanka and S. S. Sen, *Dalton Trans.*, 2017, **46**, 2420–2424.
26 C. C. Chong, H. Hirao and R. Kinjo, *Angew. Chem., Int. Ed.*, 2015, **54**, 190–194.
27 M. K. Sharma, S. Sinhababu, G. Mukherjee, G. Rajaraman and S. Nagendran, *Dalton Trans.*, 2017, **46**, 7672–7676.
28 CCDC 1848467–1848468 contain the crystallographic data for this paper. This data can be obtained free of cost from the CCDC center using the link https://www.ccdc.cam.ac.uk/.
29 *SMART: Bruker Molecular Analysis Research Tool, Version 5.618*, Bruker AXS, Madison, WI, 2000.
30 *SAINT-NT, Version 6.04*, Bruker AXS, Madison, WI, 2001.
31 *SHELXTL-NT, Version 6.10*, Bruker AXS, Madison, WI, 2000.
32 (*a*) O. V. Dolomanov, L. J. Bourhis, R. J. Gildea, J. A. K. Howard and H. Puschmann, OLEX2: A complete structure solution, refinement and analysis program, *J. Appl. Crystallogr.*, 2009, **42**, 339; (*b*) G. M. Sheldrick, *Acta Crystallogr., Sect. C: Struct. Chem.*, 2015, **71**, 3–8.